

Supplementary Information for “Single charge control of localized excitons in heterostructures with ferroelectric thin films and two-dimensional transition metal dichalcogenides”

Danjie Dai ^{ab}, Xinyan Wang ^{ab}, Jingnan Yang ^c, Jianchen Dang ^{ab}, Yu Yuan ^{ab}, Bowen Fu ^c, Xin Xie ^{ab}, Longlong Yang ^{ab}, Shan Xiao ^{ab}, Shushu Shi ^{ab}, Sai Yan ^{ab}, Rui Zhu ^{ab}, Zhanchun Zuo ^{ab}, Can Wang ^{*abd}, Kuijuan Jin ^{abd}, Qihuang Gong ^c, Xiulai Xu ^{*c}

^a Beijing National Laboratory for Condensed Matter Physics, Institute of Physics, Chinese Academy of Sciences, Beijing 100190, China

^b CAS Center for Excellence in Topological Quantum Computation and School of Physical Sciences, University of Chinese Academy of Sciences, Beijing 100049, China

^c State Key Laboratory for Mesoscopic Physics and Frontiers Science Center for Nano-optoelectronics, School of Physics, Peking University, 100871 Beijing, China

^d Songshan Lake Materials Laboratory, Dongguan, Guangdong 523808, China.

Corresponding Author

* xlxu@pku.edu.cn

* canwang@iphy.ac.cn

Supplementary sections

Supplementary Note 1. Optical microscope images before and after the transfer

Supplementary Note 2. Photoluminescence and Raman spectra of WSe₂/BFO

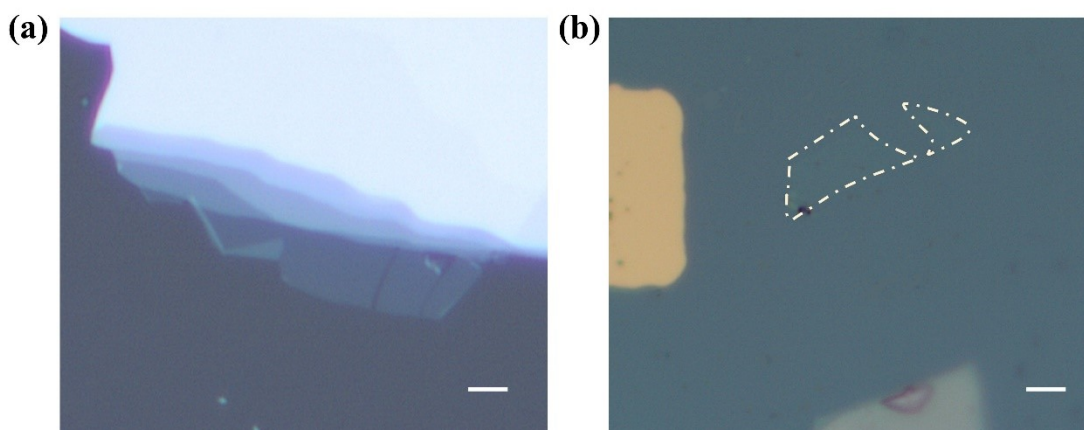
Supplementary Note 3. Polarization-resolved magneto-PL of intrinsic excitons in P_{down} and P_{up} regions

Supplementary Note 4. Linear-polarization-resolved PL of doublets in P_{dw} region.

Supplementary Note 5. Polarization-resolved magneto-PL of singlets in P_{down} and P_{up} region.

Supplementary Note 1: Optical microscope images before and after the transfer

Figure S1 illustrates the optical microscope images before and after the transfer. Figure S1(a) depicts the monolayer of WSe₂ stripped by PDMS before transfer. The optical microscope image of the monolayer transferred to the BFO film can be seen in Fig. S1(b). Even though a small portion of material is missing, same part of monolayer can be

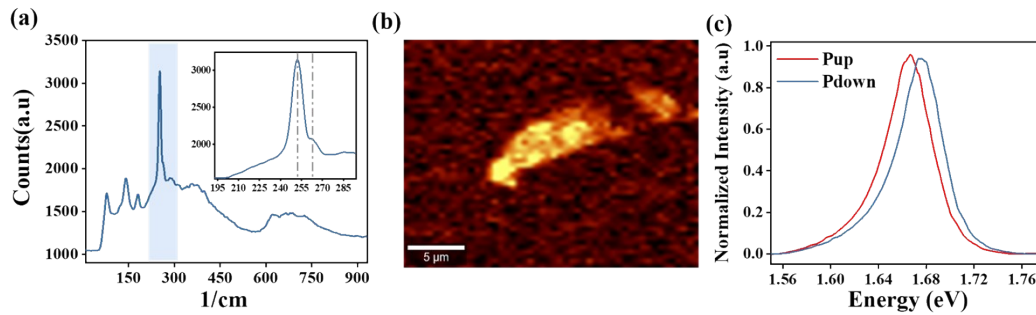


easily identified being transferred.

Figure S1 (a-b) Optical microscope images of monolayer WSe₂ before (a) and after (b) transfer. The scale bar is 3 μm .

Supplementary Note 2: Photoluminescence and Raman spectra of BFO/WSe₂

Raman spectra of BFO/WSe₂ at room temperature are shown in Fig. S2. The inset of Fig. S2(a) depicts a magnified view of two dominant peaks around 250 cm⁻¹. The E_{2g} mode at ~251 cm⁻¹ and A_{1g} modes at ~262 cm⁻¹ of WSe₂ flakes are observed, with a frequency difference of 11 cm⁻¹ between E_{2g} and A_{1g}, which is consistent with the reported frequency difference between the corresponding Raman peaks of monolayer WSe₂.¹ Raman mapping (as shown in Fig. S2(b)), monitoring the 251 cm⁻¹ Raman peak, matches well with the shape of optical microscope image, demonstrating that the WSe₂ flake was successfully transferred to the BFO. Figure S2(c) shows the PL of WSe₂ flakes at 300 K in the P_{down} and P_{up} regions. The emission peaks in the P_{down} and P_{up} regions are 1.67 and 1.66 eV, respectively, which are consistent with the PL of monolayer WSe₂ at room temperature.^{2,3} The modulation of the monolayer WSe₂ charge level by the ferroelectric polarization effect of the BFO causes a red shift in the emission

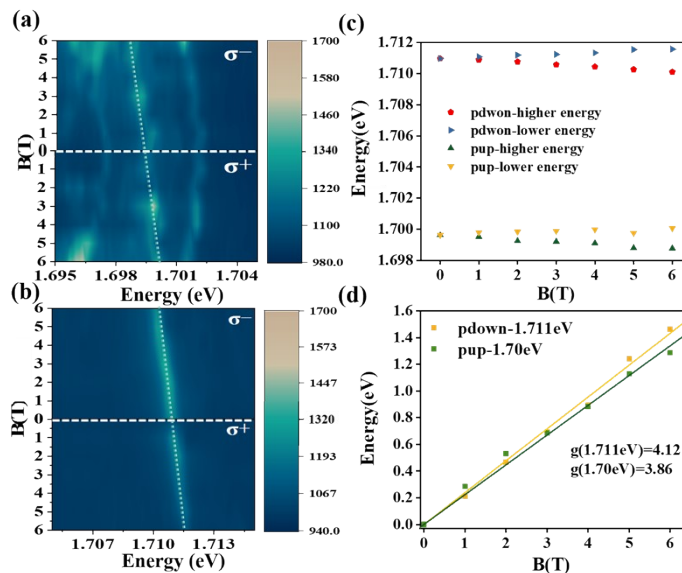


of charged excitons in the P_{up} region compared to that in the P_{down} region.

Figure S2 Raman and PL spectra of BFO/WSe₂. (a) Raman spectrum of BFO/WSe₂ at room temperature. The inset shows the details of the E_{2g} and A_{1g} modes of the monolayer WSe₂. (b) Raman mapping of BFO/WSe₂ by monitoring the 251 cm⁻¹ Raman peak. (c) PL spectra of monolayer WSe₂ in the P_{down} and P_{up} regions at room temperature.

Supplementary Note 3: Polarization-resolved magneto-PL of intrinsic excitons in P_{down} and P_{up} regions

By measuring temperature-dependent PL from 35 K to 273 K, we have shown that the doping type of direct bandgap emission of WSe₂ changes from n-type to p-type from natural polarization P_{down} region to reversed polarization P_{up} region. To further confirm that the peaks labeled in the temperature-dependent PL belong to the direct band emission, we investigated their magnetic response at 4.2 K. The polarization-resolved magneto-PL spectra of the peak at 1.70 eV in P_{up} region and the peak at 1.71 eV in P_{down} regions are shown in Fig. S3(a-b). Figure S3(c-d) reveal the energy splitting varies with the magnetic field, where the g-factor can be extracted. The g-factors of these two peaks in the

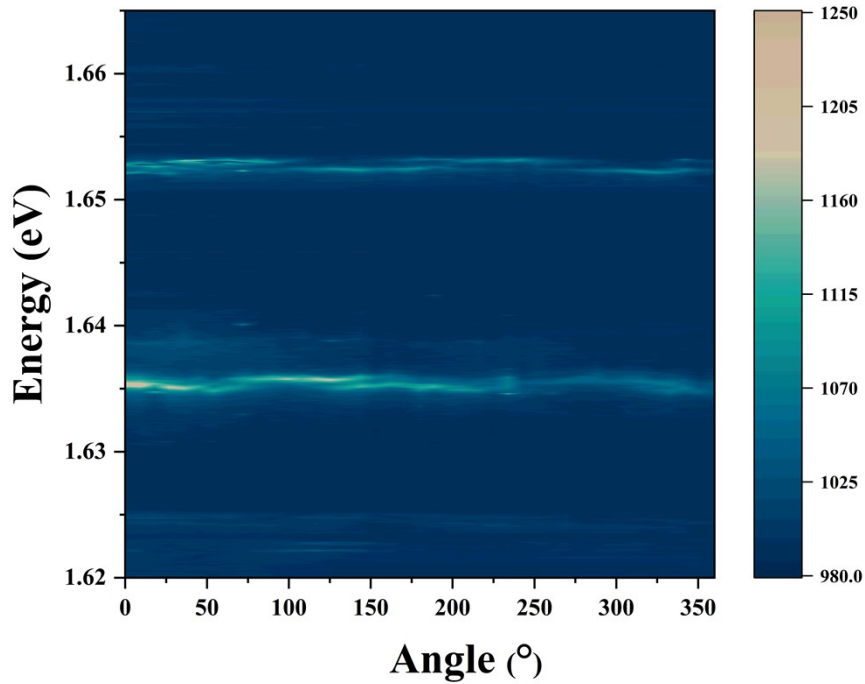


two regions are both close to 4, indicating that they belong to the direct band gap emission.

Figure S3 Polarization-resolved magneto-PL of intrinsic excitons in P_{down} and P_{up} regions in a Faraday configuration magnetic field. (a-b) Polarization resolved PL under linear excitation for σ^+ (a) and σ^- (b) collection. (c) The circular polarization degree of direct band emissions in P_{up} and P_{down} regions from (a) and (b).

Supplementary Note 4: Linear-polarization-resolved PL of doublets in the P_{dw}

It can be noted that the PL emissions of localized excitons are almost doublets in the domain wall at 4.2 K. Figure S4 displays the linear polarization PL of the doublets at the domain wall. These doublets correspond to cross-linear polarized emissions, which further indicates that the split peaks of the doublets in the domain wall at zero field originate from the same quantum dots embedded in monolayer WSe_2 . The splitting of neutral localized excitons at zero field is the result of fine structure splitting (FSS) caused by anisotropic electron-hole exchange interactions in



asymmetric confinement potentials.

Figure S4 Contour plot of linear-polarization-resolved PL spectra of doublets in the domain wall.

Supplementary Note 5: Polarization-resolved magneto-PL of singlets in P_{down} and P_{up} regions

The polarization-resolved spectra of singlets in the P_{down} and P_{up} regions are displayed in Fig. S5(a-d). It can be found that the σ^- collection shifts to lower energy, whereas σ^+ collection exhibits the opposite behavior with a blue shift with the increase of magnetic field. At zero field, the PL emission peak at P_{down} and P_{up} regions both exhibit a single peak with unresolvable FSS. The splitting between higher energy peaks and lower energy peaks becomes larger with the increasing magnetic field. To analyze the circular polarization degree of the peaks with the increase of magnetic field, Fig. S5(e-f) depict the circular polarization at different magnetic field by using:

$$P = \frac{I_{\sigma^-} - I_{\sigma^+}}{I_{\sigma^-} + I_{\sigma^+}}$$

where I_{σ^+} (I_{σ^-}) denotes the intensity of the σ^+ (σ^-) polarized emission for linearly polarized excitation. A circular polarization degree up to $\sim 80\%$ is obtained in the presence of magnetic fields.

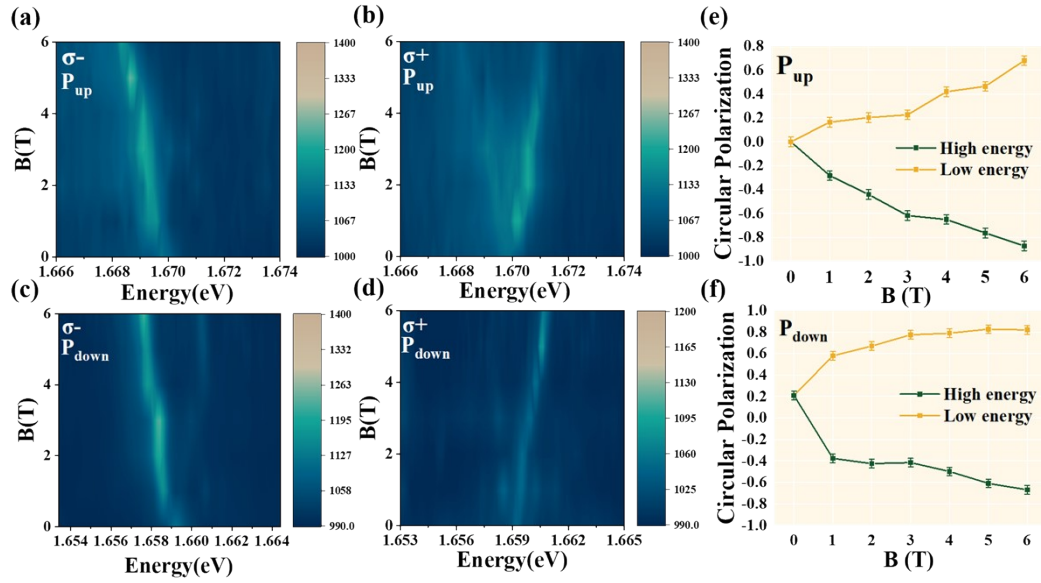


Figure S5 Polarization-resolved magneto-PL of excitons in P_{down} and P_{up} regions in a Faraday configuration magnetic field. (a-b) Polarization-resolved PL under linear excitation for σ^- (a) and σ^+ (b) collection in the P_{up} region. (c-d) Polarization-resolved PL under linear excitation for σ^- (c) and σ^+ (d) collection in the P_{down} region. (e-f) The circular polarization degree of high energy and low energy peak in P_{down} (e) and P_{up} (f) regions.

REFERENCE

1. H. Zeng, G. B. Liu, J. Dai, Y. Yan, B. Zhu, R. He, L. Xie, S. Xu, X. Chen, W. Yao and X. Cui, *Sci. Rep.*, 2013, **3**, 1608.
2. Z. Li, T. Wang, C. Jin, Z. Lu, Z. Lian, Y. Meng, M. Blei, S. Gao, T. Taniguchi, K. Watanabe, T. Ren, S. Tongay, L. Yang, D. Smirnov, T. Cao and S. F. Shi, *Nat. Commun.*, 2019, **10**, 2469.
3. E. Liu, J. van Baren, C. T. Liang, T. Taniguchi, K. Watanabe, N. M. Gabor, Y. C. Chang and C. H. Lui, *Phys. Rev. Lett.*, 2020, **124**, 196802